Crystalline structure and squeeze-out dissipation of liquid solvation layers observed by small-amplitude dynamic AFM

W. Hofbauer,* R. J. Ho, Hairulnizam R.,† N. N. Gosvami,‡ and S. J. O'Shea
*Institute of Materials Research and Engineering (IMRE), Agency for Science, Technology and Research (A*STAR), 3 Research Link, Singapore 117602, Singapore*

(Received 13 April 2009; revised manuscript received 25 June 2009; published 2 October 2009)

Using frequency-modulation atomic force microscopy (FM-AFM) at sub-nanometer vibration amplitudes, we find in the system *n*-dodecanol/graphite that solvation layers may extend for several nanometers into the bulk liquid. These layers maintain crystalline order which can be imaged using FM-AFM. The energy dissipation of the vibrating tip can peak sharply upon penetration of molecular layers. The tip shape appears critical for this effect.

DOI: 10.1103/PhysRevB.80.134104 PACS number(s): 68.08.De, 68.15.+e, 68.37.Ps

A notable property of liquid near the liquid-solid interface is the presence of solvation layers, i.e., ordering of liquid molecules due to boundary conditions imposed by the solid. Such layering has been observed via oscillatory solvation forces when confining the liquid between the substrate and a solid probe using the surface force apparatus[1] and atomic force microscopy (AFM).[2,3] While solvation forces are routinely detected via the modulation of the force, the lateral structure of the solvation shells—beyond the first adsorbed monolayer—has rarely been directly observed. One exception are long-chain alkanes adsorbed from solution, for which a second layer has been imaged using scanning tunneling microscopy (STM).[4] Unfortunately, STM does not lend itself to imaging of "higher" layers as the tunneling current decreases exponentially with the thickness of the confined (nonconductive) liquid. The lamellar structure of a second solvation layer of hexadecane was imaged recently using a tuning fork AFM.[5] There remain open questions about the structure of higher solvation layers, namely, whether they exhibit lateral order. These questions will become increasingly important for high-resolution AFM imaging in liquid, in particular, for hydration layers in biological systems.[6,7]

The development of instrumentation capable of small-amplitude, frequency-modulated AFM (FM-AFM) (Ref. 8) in liquid environments[9] has dramatically increased the resolution and sensitivity achievable in AFM studies in liquid. We apply FM-AFM to a linear alcohol (dodecanol) on an atomically flat graphite substrate slightly above the bulk freezing temperature. We find not only spectroscopic evidence of multiple solvation layers, i.e., force oscillations but also obtain real-space topography images of the alcohol molecules in higher layers, demonstrating that the solvation layers in this system have a crystalline structure. Further we sometimes observe, depending on the condition of the tip, sharp peaks in the mechanical dissipation just as a solvation layer is squeezed out of the tip-sample gap.

To achieve the sensitivity necessary for molecular resolution AFM in liquid, a commercial AFM (Molecular Imaging Picoscope) was modified. Changes to the optical beam deflection sensor include replacement of the standard laser source with a home-built, rf-modulated diode laser[9] and modification of the focusing optics to achieve a smaller numerical aperture. Using standard silicon cantilevers (type NCLR, Nanosensors, Neuchatel, Switzerland and type ACLA, AppNano, Santa Clara, CA) with a spring constant of $k_c \approx 40$ N/m, a deflection noise density of <40 fm/$\sqrt{\text{Hz}}$ in water was estimated from the thermal noise spectrum.[8] Experiments were performed at a cantilever vibration peak-to-peak amplitude of $A_{pp} \approx 0.25$ nm (0.09 nm rms).

Direct magnetic excitation[10] of the cantilever was employed to eliminate parasitic resonances common with other excitation schemes. Such parasitic resonances usually result in gross errors in amplitude and phase determination in dynamic AFM methods.[11,12] Commercial silicon cantilevers (see above) were modified by gluing a spherical magnetic bead (MQP-S-11-9 isotropic rare-earth magnet powder, Magnequench, Singapore) to the backside.[13] The modified cantilevers were subsequently magnetized in an external 1 T field parallel to the cantilever axis. The sample holder plate was fitted with a low-inductance (≈ 30 μH) ferrite-core solenoid to generate a driving magnetic field from below the sample with sufficient bandwidth.

With these modifications, clean Lorentzian cantilever resonance curves were routinely obtained. The elimination of spurious resonances also allows one to omit a bandpass preselector filter[9] that would result in additional phase errors. Due to the added bead mass and hydrodynamic loading, the cantilever resonance frequencies in liquid are on the order of $f_0 \approx 50$ kHz.

The cantilever resonance was tracked and driven by a phase-locked loop (PLLpro, RHK Technology, Troy, MI). The frequency shift can be directly related to conservative forces acting on the tip. All images were obtained using constant frequency-shift topography feedback. The drive amplitude was regulated to maintain a constant vibration amplitude A_{pp}; the drive amplitude therefore corresponds directly to the dissipation of the cantilever vibration (assuming the oscillations are harmonic).

The per-cycle energy dissipation E_d at resonance scales with the driving force F_d (or, for magnetic excitation, the drive current), $E_d \propto A_{pp} F_d$, independent of frequency. Considering that the quality factor is $Q = 2\pi E / E_d$ (where E is the steady-state oscillator energy), the dissipation can be determined from the driving force $F_{d,0}$ and the quality factor Q_0 obtained away from the surface,

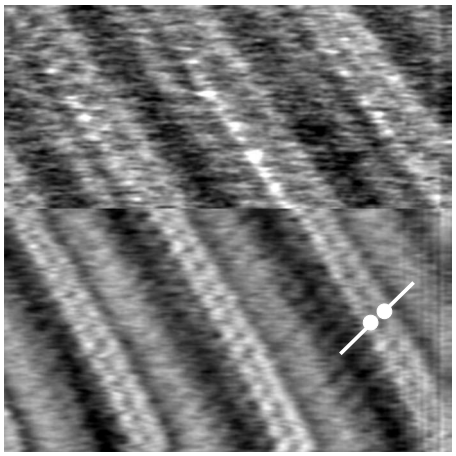

FIG. 1. High-resolution topography (bottom) and dissipation (top) image (20×20 nm^2, $\Delta f=5.4$ kHz, linear scan speed 500 nm/s) of a solvation layer of *n*-dodecanol on HOPG. Submolecular features such as the OH headgroups are clearly discernible.

$$E_{\mathrm{d}} = \frac{\pi k_{\mathrm{c}} A_{\mathrm{pp}}^2}{4Q_0} \frac{F_{\mathrm{d}}}{F_{\mathrm{d},0}}. \tag{1}$$

Freshly cleaved highly ordered pyrolytic graphite (HOPG SPI-2 grade, SPI supplies, West Chester, PA) was used as a solid substrate and covered ≈ 3 mm deep with *n*-dodecanol (*puriss.* >98.5%, Fluka). The liquid cell was open and not sealed against ambient. Experiments were performed at ≈ 25 °C, slightly above the dodecanol bulk freezing temperature of ≈ 23 °C.

We routinely obtained AFM images of dodecanol molecules arranging side-by-side in a lamellar pattern. Depending on the condition of the tip and the chosen frequency-shift setpoint (typically a few hundred Hz to a few kHz), submolecular features could be resolved in the topography image (Fig. 1). Similar images of adsorbed monolayers of a wide range of linear molecules have been extensively studied by STM.[14,15]

During the acquisition of the image in Fig. 2, the frequency-shift setpoint was slowly varied. As the setpoint changes, the topography changes in discrete steps of ≈ 0.45 nm in the vertical (z) direction, reflecting six successive solvation layers of dodecanol molecules. The dissipation image shows similar features, with higher dissipation corresponding to layers closer to the substrate. It is apparent that imaging is possible for layers up to several nanometers away from the solid surface.

From the "flattened" image (i.e., after baseline subtraction), it can be seen that the lateral (x,y) ordering of the molecules is also maintained up to several nanometers away from the surface. In other words, the "liquid" molecules exhibit crystalline order in the vicinity of the graphite substrate, extending for several nanometers into the "bulk" liquid. Surface-induced crystallization has been predicted by molecular-dynamics simulations of alkanes,[16–18] but has not been previously imaged directly. It also has been suggested that solidification of nanoconfined liquids may be a kinetic effect dependent on the approach speed of an oscillating AFM tip.[3] However, when imaging a layer as in our case, the

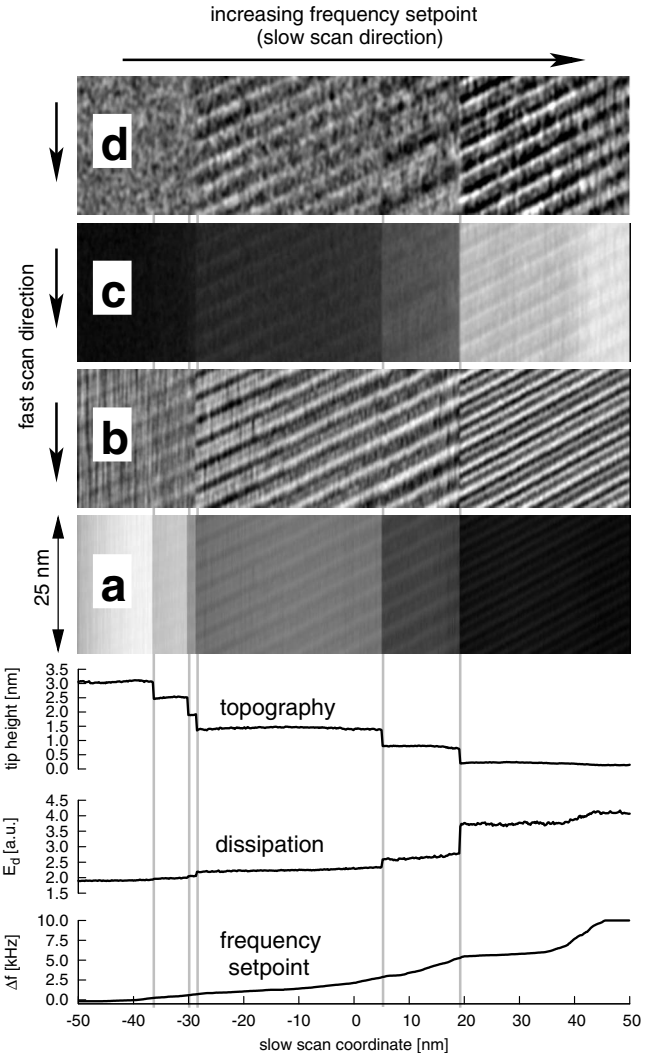

FIG. 2. Simultaneously acquired 100 nm$\times$25 nm AFM image data of *n*-dodecanol on HOPG obtained while varying the frequency-shift setpoint (a: topography, b: flattened topography, c: dissipation, and d: flattened dissipation). Note that the scan axes are shown rotated by 90° compared to the typical AFM image view. The equidistant jumps in height reflect the tip controlling in six successive solvation layers. A well-ordered lateral structure is maintained throughout the layers. Bottom: topography profile, dissipation profile, and frequency-shift setpoint along the slow scan axis of the AFM image.

tip height is essentially fixed and the approach rate is zero (apart from the submolecular scale vibration of the tip). It is an open question whether the lateral tip movement during imaging could contribute, via shear-induced alignment,[19] to the observed molecular ordering.

Figure 3 shows the simultaneous frequency shift, dissipation, and quasistatic cantilever deflection as a function of relative[20] tip-sample separation as the tip approaches the surface. Similar data are obtained when the tip is subsequently retracted. The increase in stiffness and dissipation (effectively, the viscosity) at small separations has been observed previously.[2] However, there are several new aspects to note. First, the ability to image long-range, crystalline order is one simple definition of a solid.[21] Thus, imaging an ordered

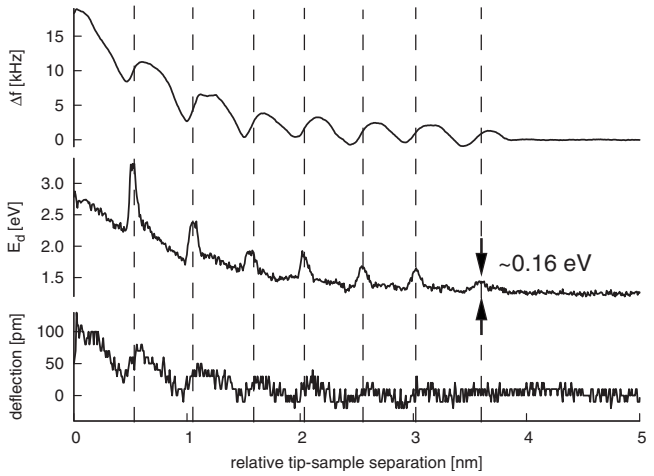

FIG. 3. Simultaneous frequency shift, dissipation, and static cantilever deflection during a tip approach (approach rate 1 nm/s). The oscillatory nature of the solvation force is clearly observed in the frequency shift. The dissipation peaks whenever a molecular layer is squeezed out. The origin of the separation axis is arbitrary (Ref. 20).

structure within a solvation layer can be regarded as evidence that the particular layer is solid. Such information can be correlated with force curve measurements, the only AFM technique available previously, to address contentious issues such as the occurrence of confinement-induced phase transitions[18] and whether a confined material is a solid or liquid.[3]

It is also worth noting that a sudden onset of layering is observed at a certain separation (at ≈3.7 nm in Fig. 3). There appears to be a distinct phase boundary between the layered and the unordered liquid state, rather than a gradual decay of molecular order into the bulk liquid. This observation may show the predicted transition from liquid to solid behavior at a specific solvation layer separation[18] induced by the confinement of the liquid between two surfaces. At present we cannot confirm that images showing crystalline structure (e.g., Fig. 1) can be taken in the solvation layer(s) furthest from the surface. This is because constant frequency imaging, combined with a nonmonotonic force curve, leads to uncertainty as to which solvation layer the tip is controlling within. However, we note that the number of crystalline layers seen in variable-setpoint topographic imaging (e.g., Fig. 2) is comparable to the number of layers found in force curve experiments (Fig. 3).

Another intriguing observation is the periodic peaking of the dissipation signal. Nonmonotonic modulation of the dissipation signal can arise as an artifact from phase errors that lead to mixing of frequency shift and dissipation signals.[11,12,22] We rule out this possibility on several grounds: (i) the clean resonance curves obtained using magnetic cantilever actuation minimize the chance of gross phase (tuning) errors; (ii) the features of the dissipation signal are distinctly narrower than those of the frequency-shift signal; and (iii) the dissipation features persist at reduced approach rates (0.5 nm/s) while using very high PLL feedback gain, eliminating insufficient transient response of the PLL as a cause for artifacts.

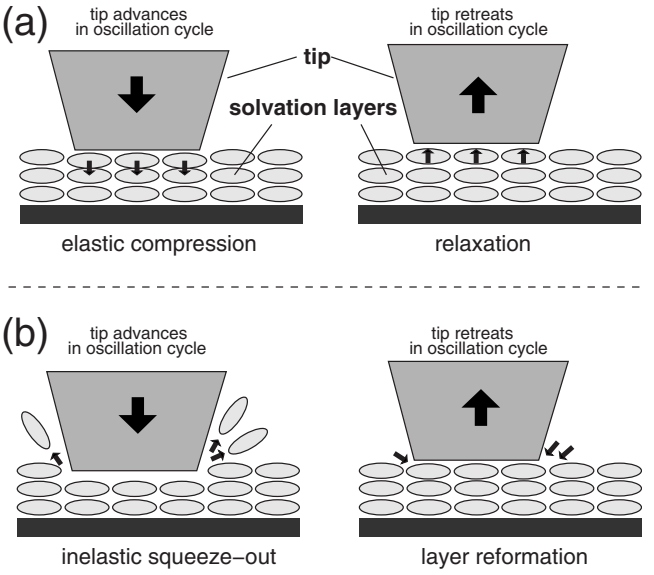

FIG. 4. Schematic of two different regimes for the dissipation of vibration energy of an oscillating AFM tip. (a) There is no removal of solvation layers in the oscillation cycle. Cyclic elastic compression results in minimal reconfiguration of molecules, giving high stiffness with low dissipation. (b) A solvation layer is expelled from the tip-sample gap in the oscillation cycle. Cyclic squeeze out (penetration) and reformation of a layer incurs increased dissipation. Also, as the molecules give way, the interfacial stiffness is relaxed.

In related work using octamethyltetrasiloxane,[3] oscillatory behavior of dynamic stiffness and dissipation was reported to occur either in phase or antiphase as the separation varied, and explained as a result of solidification at different tip approach rates. In our case, the shape of the frequency shift (i.e., stiffness) and dissipation signals are rather dissimilar (Fig. 3) and the images show the confined material is crystalline even when the tip height is stationary (Fig. 2), calling for another explanation.

A plausible model for the nonmonotonic dissipation curve assumes two alternating dissipation mechanisms in the small-amplitude regime (Fig. 4). In one case [Fig. 4(a)], the modulation of mechanical stress exerted by the vibrating tip leads to periodic compression and decompression of the underlying molecular lattice. As the molecular order is maintained and no large-scale molecular movement is involved, this process is dominated by the elastic, low-dissipation response characteristic of a crystalline solid. In the second case [Fig. 4(b)], the compression is increased to the point where layer penetration occurs. At this point the vibrating tip is repeatedly expelling and reincorporating molecules within a solvation layer in every oscillation cycle. This squeeze-out process[23] relaxes the mechanical stress and lowers the effective sample stiffness sensed by the tip, but results in increased dissipation. Possible dissipation mechanisms include viscous flow of the displaced molecules as well as mechanically induced breakup (during tip advance) and exothermic reassembly (during tip retreat) of the molecular layer. This model is consistent with the frequency-shift data, which indicate reduced dynamic stiffness in the regions of enhanced dissipation as the molecules "give way," and by the static

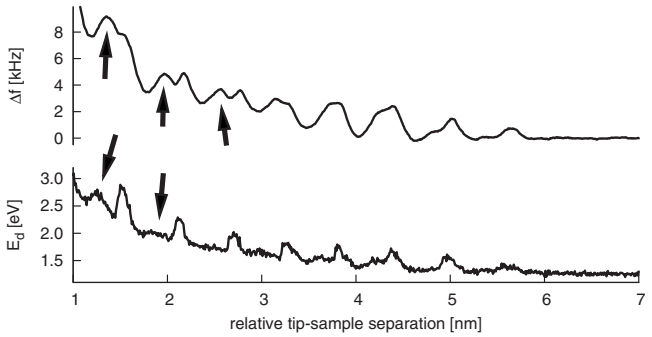

FIG. 5. Frequency shift and dissipation spectra for an AFM tip with a secondary-tip asperity. During tip approach, the first asperity gives rise to oscillatory solvation force features. When approaching further, the second asperity comes into contact with the solvation layers, superimposing another set of squeeze-out signatures (arrows) on the spectra.

cantilever deflection, which shows that the low-dissipation regions coincide with a reduction in stress on the sample, i.e., layer penetration.

The squeeze out of the solvation layers is generally considered a collective process involving many molecules, both for crystalline and liquid layers where some activation volume is associated with the viscous flow.[23–26] It is therefore difficult to relate the dissipation data to individual molecular-scale events. With this caveat, and neglecting viscous-flow contributions, one may consider the dissipation of 0.16 eV $\approx 6k_BT$ per cycle measured for the outermost layer as a rough gauge for the binding energy of a small number of layered molecules. In this interpretation, the per-molecule energy is so close to the thermal activation limit that it would explain the abrupt termination of molecular order away from the HOPG surface at a phase boundary (Fig. 3). We note that the data associated with the layers closer to the substrate cannot be analyzed in the same simple manner. This is because for the outermost layer only the tip apex is interacting with the crystalline outer layer, and the dissipation acting on the rest of the tip in the bulk liquid is constant with distance. However, as the tip is immersed within the layered region, more than one specific layer may contribute to the measured dissipation. So, with the exception of the outermost layer, the data is probably not a simple reflection of dissipation in a *single* layer.

We found that while the molecular structure can be imaged routinely (e.g., Fig. 1), the presence of the sharp dissipation features depends to a large extent on the individual tip. For most tips, the dissipation peaks appeared much smoother or were not noticeable at all. We also found dissipation peaks could be induced after deliberately blunting one tip by scanning in contact mode. In a final example, when a tip apex consists of microasperities of similar height, one might expect discrete copies of spectral features to be superimposed on the smooth background. We observed circumstantial evidence of this phenomenon on several occasions. In Fig. 5 it can be seen how, on approaching the substrate, the forces on the tip are modulated by the layered structure of the liquid. As the separation decreases further, a second microasperity comes into contact with the solvation layers, contributing another oscillatory force component and leading to an apparent splitting of peaks in the frequency and dissipation spectra.

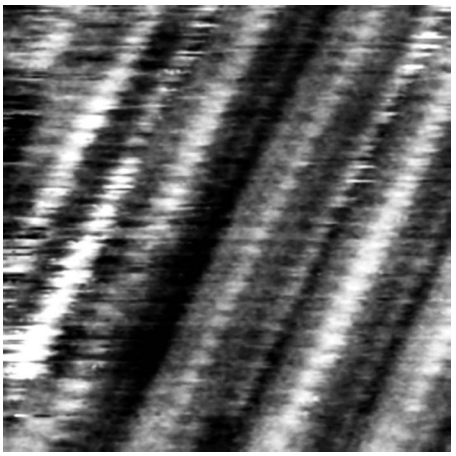

FIG. 6. Topography image ($\approx 20 \times 20$ nm^2) obtained using a deliberately worn AFM tip. The apparent molecular resolution may be due to lattice averaging and/or the existence of atomic-scale asperities.

Note that the bluntness of a tip does not necessarily correlate with the observed lateral image resolution. Molecular resolution can be retained by the existence of atomic-scale asperities protruding from the tip apex or, in the case of a periodic structure as in our case, by averaging over multiple molecules, i.e., lattice-resolution imaging. For example, Fig. 6 shows an image of a solvation layer taken with the same tip used for Fig. 5. While the image quality is degraded, molecular-scale resolution can still be discerned.

Thus it is difficult to directly test our conjecture that blunter tips influence the appearance of dissipation peaks because we cannot find the tip shape from the measured images. We can only infer that the microasperities are the underlying cause of the changes in the dissipation peaks (e.g., Fig. 5) from the force curves and the observation that blunt tips preferentially show such behavior. Even transmission electron microscopy will not assist greatly as it is very difficult to image ~1-nm-sized asperities on a tip apex. Nevertheless, the influence of multiple asperities on AFM solvation force measurements is known, at least qualitatively,[27] and for very blunt tips (radius of curvature >50 nm) microasperities or irregular tip geometry almost certainly exist.[28]

The above comments emphasize the significance of the nanoscale tip shape in AFM.[29] We propose that the tip shape is also critical to the dynamics of solvation layer squeeze out and may be the underlying cause of the variability and differing "features" observed in AFM dissipation data. For example, oscillations in the dissipation signal have been reported for octamethyltetrasiloxane on HOPG using gold coated silicon tips[3] but not for ultrasharp silicon tips[2] or carbon nanotube tips.[30] Whether tip size effects depend on the distance over which molecules act cooperatively during squeeze out[25] requires further experimentation.

In summary, we have shown that *n*-dodecanol on HOPG forms well-ordered, crystalline solvation layers above the bulk melting point, with a sharp boundary between bulk and

layered phases. Small-amplitude dynamic AFM is not only able to image these ordered layers with submolecular resolution, but also identifies two different dissipation regimes during squeeze out of molecular layers. Finally, we note that we observe similar dissipation behavior in *n*-hexadecane on HOPG, indicating that the dissipation mechanism may be applicable to a wider range of layering liquids, although the effect of tip shape must be considered further.

*wulf-h@imre.a-star.edu.sg
†Also at Department of Mechanical Engineering, National University of Singapore.
‡Present address: Leibniz-Institut für Neue Materialien, 20 Campus D2 2, D-66123 Saarbrücken, Germany.

[1] R. G. Horn and J. N. Israelachvili, J. Chem. Phys. **75**, 1400 (1981).
[2] S. J. O'Shea and M. Welland, Langmuir **14**, 4186 (1998).
[3] S. Patil, G. Matei, A. Oral, and P. M. Hoffmann, Langmuir **22**, 6485 (2006).
[4] G. Watel, F. Thiebaudau, and J. Cousty, Surf. Sci. Lett. **281**, L297 (1993).
[5] L. P. Van, V. Kyrylyuk, J. Polesel-Maris, F. Thoyer, C. Lubin, and J. Cousty, Langmuir **25**, 639 (2009).
[6] T. Fukuma, M. Higgins, and S. P. Jarvis, Biophys. J. **92**, 3603 (2007).
[7] M. J. Higgins, M. Polcik, T. Fukuma, J. E. Sader, Y. Nakayama, and S. P. Jarvis, Biophys. J. **91**, 2532 (2006).
[8] T. Albrecht, P. Grütter, D. Horne, and D. Rugar, J. Appl. Phys. **69**, 668 (1991).
[9] T. Fukuma, M. Kimura, K. Kobayashi, K. Matsushige, and H. Yamada, Rev. Sci. Instrum. **76**, 053704 (2005).
[10] S. J. O'Shea, M. Welland, and J. Pethica, Chem. Phys. Lett. **223**, 336 (1994).
[11] S. J. O'Shea, Phys. Rev. Lett. **97**, 179601 (2006).
[12] G. B. Kaggwa, J. I. Kilpatrick, J. E. Sader, and S. P. Jarvis, Appl. Phys. Lett. **93**, 011909 (2008).
[13] Donation of a MQP-S-11-9 sample by Magnequench Singapore is gratefully acknowledged.
[14] L. C. Giancarlo and G. W. Flynn, Annu. Rev. Phys. Chem. **49**, 297 (1998).
[15] J. P. Rabe and S. Buchholz, Science **253**, 424 (1991).
[16] R. Hentschke, B. L. Schürmann, and J. P. Rabe, J. Chem. Phys. **96**, 6213 (1992).
[17] T. Yamamoto, K. Nozaki, A. Yamaguchi, and N. Urakimi, J. Chem. Phys. **127**, 154704 (2007).
[18] S. T. Cui, P. T. Cummings, and H. D. Cochran, J. Chem. Phys. **114**, 7189 (2001).
[19] C. Drummond, N. Alcantar, and J. Israelachvili, Phys. Rev. E **66**, 011705 (2002).
[20] The absolute tip-sample separation can be found by increasing the force to the point of substrate contact. However, the rather large forces necessary would result in undesirable changes to the tip.
[21] W. D. Kaplan and Y. Kauffmann, Annu. Rev. Mater. Res. **36**, 1 (2006).
[22] J. E. Sader and S. P. Jarvis, Phys. Rev. B **74**, 195424 (2006).
[23] B. N. J. Persson and F. Mugele, J. Phys.: Condens. Matter **16**, R295 (2004).
[24] U. Tartaglino and I. M. Sivebaek, J. Chem. Phys. **125**, 014704 (2006).
[25] H.-W. Hu, G. A. Carson, and S. Granick, Phys. Rev. Lett. **66**, 2758 (1991).
[26] A. L. Demirel and S. Granick, Phys. Rev. Lett. **77**, 2261 (1996).
[27] R. Lim, S. F. Y. Li, and S. J. O'Shea, Langmuir **18**, 6116 (2002).
[28] L. T. W. Lim, A. T. S. Wee, and S. J. O'Shea, Langmuir **24**, 2271 (2008).
[29] B. Luan and M. O. Robbins, Nature (London) **435**, 929 (2005).
[30] T. Uchihashi, M. Higgins, Y. Nakayama, J. E. Sader, and S. P. Jarvis, Nanotechnology **16**, S49 (2005).